Journal of Chromatography, 260 (1983) 225–239
Elsevier Science Publishers B.V., Amsterdam — Printed in the Netherlands

CHROM. 15,664

ANALYTICAL ISOTACHOPHORESIS UTILIZING COMPUTER SIMULATION

I. FACTORS AFFECTING THE QUANTITATIVE INDICES AND UTILITY FOR DETERMINATIONS

TAKESHI HIROKAWA* and YOSHIYUKI KISO
Applied Physics and Chemistry, Faculty of Engineering, Hiroshima University, Shitami, Saijo, Higashi-hiroshima 724 (Japan)
(Received January 3rd, 1983)

SUMMARY

Factors affecting a quantitative index in isotachophoresis, namely time-based zone length, t, and the gradient of the conventional calibration line, are discussed. Simple equations for the estimation of t have been derived for mono- and divalent anions, and the deviation from the accurately simulated values plotted for model mono- and divalent anions. The observed zone lengths have been compared with the accurately simulated ones for actual samples. Satisfactory agreement was achieved and the practical utility of the simulation technique was confirmed.

INTRODUCTION

By means of isotachophoresis, qualitative and quantitative determinations of ionic species can be made by analysing ratios of step heights, for example R_E values, and time-based zone lengths, respectively. As reported previously[1], at an isotachophoretically steady state these values can be calculated with the aid of a computer if the absolute mobilities and thermodynamic dissociation constants of the system constituents are known. The qualitative index, R_E, was discussed in detail in previous papers[1,2].

In this paper, the quantitative index, *i.e.*, time-based zone length, t, is treated theoretically to clarify factors affecting it and the meaning of the coefficient of proportionality in calibration curves of t *vs.* sample amount, n. Beckers and Everaerts[3] had previously proposed a calibration constant, K_{cal}. We will consider this constant in a later section.

The simulational calculation for the general case is rather complicated[1] owing to the need to make certain corrections, *e.g.*, for the effect of ionic strength on mobility and dissociation constants. Therefore simple equations to estimate the approximate zone length were derived for monovalent and divalent ions. These estimates for several model anions were then compared with the accurately evaluated ones to show the limitations of the simple equations.

0021-9673/83/$03.00

Finally, the accurately simulated zone lengths and the coefficients of proportionality were compared with the observed[3] values for several anions to confirm the utility of the simulational technique in determinations.

THEORETICAL

In isotachophoresis, the total concentration of a separated sample, C_S^l, is usually different from the concentration of the injected sample. C_S^l (mol/l) is regulated by the Kohlrausch function at a steady state and it is usually smaller than the total concentration of a leading ion. The zone length of the separated sample, l (cm), can be expressed as

$$l = 1000\, n/C_S^l\, \pi\, r^2 \tag{1}$$

where r (cm) is the inner radius of the separating tube and detector used and n (mol) is the sample amount. The time-based zone length, t (sec), is equal to the actual zone length divided by the isotachophoretic velocity, v (cm/sec)

$$t = 1000\, n/C_S^l\, \pi\, r^2\, v \tag{2}$$

$$v = E_L\, \bar{m}_L = E_S\, \bar{m}_S \tag{3}$$

where E (V/cm) and $\bar{m}$ (cm^2/V · sec) are the potential gradient and the effective mobility, respectively. The subscripts L and S denote the leading and the sample zones (ions). Combining eqns. 1–3 gives

$$t = 1000\, n/C_S^l\, \pi\, r^2\, E_S\, \bar{m}_S \tag{4}$$

$$E_S = J/\kappa_S = I/\pi\, r^2\, \kappa_S \tag{5}$$

where J (A/cm^2) is the current density, I (A) the applied driving current and κ_S (S/cm) the specific conductivity of the separated zone. Then, t can be expressed generally:

$$t = 1000\, n\, \kappa_S/I\, C_S^l\, \bar{m}_S \tag{6}$$

From eqn. 6, the coefficient of proportionality between n and t can easily be obtained, and is conventionally used in practical quantitative analysis. It should be noted that t is not affected by the dimensions of the detector used, contrary to l.

For the evaluation of t for a given amount n using eqn. 6, κ_S, C_S^l and $\bar{m}_S$ at an isotachophoretically steady state must be simulated. κ_S can be expressed exactly as

$$\kappa_S = \left(C_{H,S}\, m_H + C_{OH,S}\, m_{OH} + \sum_{i=0}^{n_S} \left| Z_S - i \right| C_{Z_S - i}\, m_{Z_S - i} + \sum_{i=0}^{n_B} \left| Z_B - i \right| C_{Z_B - i,S}\, m_{Z_B - i} \right) \times F/1000 \tag{7}$$

where $C_{H,S}$ is the concentration of H^+ in the sample zone, m_H the effective mobility of H^+, $C_{OH,S}$ the concentration of OH^-, m_{OH} the mobility, C_{Z_S-i} the concentration of ionic component of a sample with charge $Z_s - i$, m_{z_s-i} the mobility (similar expressions with subscripts B being for the buffer ion) and F the Faraday constant. Eqn. 7 can be adopted for any multivalent sample and buffer ions at any pH_L. Under certain conditions, eqn. 7 can be reduced to a more simple form. Namely, in the medium pH range, the contribution of H^+ and OH^- to κ_S is negligibly small, thus the related terms can be ignored. When the sample and the buffer are monovalent, eqn. 7 reduces to

$$\kappa_S = (C_S m_S + C_{B,S} m_{B,S}) F/1000 \tag{8}$$

where C and m are the concentration and the mobility of the ionic components, and the subscripts S and B denote the sample ions (or zones) and the buffer ions; $m_{B,S}$ is the mobility of the buffer ion in the sample zone. It should be noted that m_S and m_B are the mobilities in an electrolyte with a finite ionic strength regulated by isotachophoretic equilibria, namely, they are smaller than the absolute mobilities. In the range pH 4–10, C_S is equal to C_B, as is apparent from the electroneutrality relationship. Inserting eqn. 8 and the relation $\bar{m}_S = C_S m_S / C_S^t$ into eqn. 6 gives:

$$t = F n (1 + m_B/m_S)/I \tag{9}$$

In eqn. 9, $1 + m_B/m_S$ corresponds to the reciprocal of the transport number of the sample ion. It is seen that t is not affected by the pK_a of the sample or pH_L, and when I and n are constant, t is uniquely determined by the ratio of the mobilities. Apparently, the efficiency of the applied driving current for migration of a sample zone is higher in electrolyte systems containing a buffer ion with low mobility.

For the exact evaluation of t the mobilities corrected for the ionic strength of the separated zones are necessary. These values can be calculated using Onsager's equation when the ionic strength can be simulated. However, for the rough estimation of t, this correction can be neglected to a first approximation. Thus, t may be estimated conveniently by using the absolute mobilities, which can be found in the literature. In later sections, the deviation of the approximate t values from the exactly simulated values will be investigated for model anions using several buffers with different mobilities.

When the sample is a divalent ion and the buffer is monovalent, in the medium pH range κ_S can be expressed as

$$\begin{aligned}\kappa_S &= (m_{S,1} C_{S,1} + 2 m_{S,2} C_{S,2} + m_{B,S} C_{B,S}) F/1000 \\ &= [(\alpha_1 m_{S,1} + 2\alpha_2 m_{S,2}) C_S^t + \alpha_B m_{B,S} C_{B,S}^t] F/1000\end{aligned} \tag{10}$$

where the subscripts 1 and 2 denote the monovalent and divalent components of the ionic species, α the degree of dissociation and the superscripts t the total concentration of the sample and the buffer.

Taking into account the electroneutrality relationship in a separated zone (pH 4–10), we can derive the following relationship:

$$(\alpha_1 + 2\alpha_2)C_S^t = \alpha_B C_{B,S}^t \quad (11)$$

Inserting eqn. 11 to eqn. 10, κ_S can be rewritten as:

$$\kappa_S = [\alpha_1(m_{S,1} + m_{B,S}) + 2\alpha_2(m_{S,2} + m_{B,S})]\, C_S^t\, F/1000 \quad (12)$$

The $\bar{m}_S$ of the divalent anion can be expressed as:

$$\begin{aligned} \bar{m}_S &= (m_{S,1}\, C_{S,1} + m_{S,2}\, C_{S,2})/C_S^t \\ &= \alpha_1 m_{S,1} + \alpha_2 m_{S,2} \end{aligned} \quad (13)$$

Inserting eqns. 12 and 13 into eqn. 6, the time-based zone length can be expressed as

$$t = \frac{Fn[\alpha_1(m_{S,1} + m_{B,S}) + 2\alpha_2(m_{S,2} + m_{B,S})]}{I(\alpha_1 m_{S,1} + \alpha_2 m_{S,2})} \quad (14)$$

where α_1 and α_2 can be correlated:

$$\alpha_2 = \alpha_1 K_2 / C_{H,S} \quad (15)$$

Here K_2 is the dissociation constant of the divalent component and $C_{H,S}$ the H^+ concentration in the sample zone.

Introducing a ratio $\beta_2 = m_{S,2}/m_{S,1}$ and inserting eqn. 15 into eqn. 14, we obtain:

$$t = \frac{Fn}{I}\left[1 + \frac{m_{B,S}}{m_{S,1}} \cdot \frac{\left(1 + \frac{2K_2}{C_{H,S}}\right)}{\left(1 + \frac{\beta_2 K_2}{C_{H,S}}\right)} + \frac{\frac{\beta_2 K_2}{C_{H,S}}}{\left(1 + \frac{\beta_2 K_2}{C_{H,S}}\right)}\right] \quad (16)$$

Assuming that $m_{S,2}$ is twice as large as $m_{S,1}$ ($\beta_2 = 2$), eqn. 16 reduces to:

$$t = \frac{Fn}{I}[1 + m_{B,S}/m_{S,1} + 1/(1 + C_{H,S}/2\,K_2)] \quad (17)$$

$$C_{H,S}/2\,K_2 = 10^{(pK_2 - pH_S - 0.301)} \quad (18)$$

Thus, in the case of divalent samples with $\beta_2 = 2$, t is affected by the ratio $m_{B,S}/m_{S,1}$, pK_2 of the sample and pH_S. Seemingly it is not affected by pK_1; however, it is slightly affected by pK_1, since pH_S related to pK_1 in the lower pH_L range (see below). Eqn. 18 has a simple form; however, it contains pH_S ($> pH_L$), which is difficult to estimate without the aid of a computer. Nevertheless, by the use of pH_L instead of pH_S, the zone lengths can be estimated roughly as shown later.

Taking into account the above formulation, in the general case t can be expressed as

$$t = \frac{F n}{I}\left[1 + \frac{m_{B,S}}{m_{S,1}} \cdot \frac{\left(1 + \frac{2K_2}{C_{H,S}} + \frac{3K_2K_3}{C_{H,S}^2} + \cdots\right)}{\left(1 + \frac{\beta_2 K_2}{C_{H,S}} + \frac{\beta_3 K_2 K_3}{C_{H,S}^2} + \cdots\right)} + \frac{\left(\frac{\beta_2 K_2}{C_{H,S}} + \frac{2\beta_3 K_2 K_3}{C_{H,S}^2} + \cdots\right)}{\left(1 + \frac{\beta_2 K_2}{C_{H,S}} + \frac{\beta_3 K_2 K_3}{C_{H,S}^2} + \cdots\right)}\right] \quad (19)$$

where $\beta_i = m_{S,i}/m_{S,1}$.

RESULTS AND DISCUSSION

All of the simulational calculations below were carried out using a Sord microcomputer, M223 Mark III. The figures were plotted using a Watanabe x–y plotter, WX4671.

To confirm the relationship 9, first the time-based zone lengths were simulated together with the R_E values for several monovalent model anions with absolute mobilities of 20–70 · 10^{-5} cm^2/V · sec and pK_a values of −2 and 4.5. The simulation was carried under the assumptions that the amount of sample is 100 nmol and the driving current is 100 μA. The zone lengths for the different amounts can easily be calculated as t is proportional to the sample amount. The concentration of leading ion, Cl^-, is 0.01 mol/l buffered with β-alanine (Ala, pH_L 2.7–4), ε-aminocaproic acid (AMC, pH_L 3.9–4.8), creatinine (Cre, pH_L 4.7–5.3), histidine (His, pH_L 5.2–6.6), imidazole (Im, pH_L 6.5–7.6), N-tris(hydroxymethyl)aminomethane (Tris, pH_L 7.5–8.5) and 2-amino-2-methyl-1,3-propanediol (amediol, Am, pH_L 8.4–9.2). The physico-chemical constants of the samples and the buffers used in the simulations are listed in Table I. The mobilities and pK_a values were taken from the literature[4–6], except for several mobilities which were determined isotachophoretically[7].

Fig. 1 shows the pH_L dependence of the simulated R_E indexes. For the anions with pK_a 4.5 (solid curves), the R_E values increased rapidly in the lowe pH_L range due to the decrease in effective mobility. On the other hand, for the anions with pK_a −2 (broken lines), the R_E values were almost constant in the range pH_L 2.7–9.2, suggesting that they are strongly affected by m_0, sample pK_a and pH_L. However, the effect of the mobility of the buffer ion was only slight, as is apparent in the medium pH_L range of 6.5–9.2 buffered by Im (m_0 = 52 · 10^{-5} cm^2/V · sec), Tris (29.5 · 10^{-5} cm^2/V · sec) and Am (29.5 · 10^{-5} cm^2/V · sec). The curves are approximately continuous.

Fig. 2 shows the pH_L dependence of the time-based zone lengths of the model anions. Apparently, the curves are discontinuous for the same model anion, suggesting that the zone lengths are strongly affected by the buffer species, strictly, by the m_0 of the buffer. For the pH_L range buffered by Im, t for the sample with m_0 = 20 · 10^{-5} cm^2/V · sec is not shown in Fig. 2: it was *ca.* 363 sec. As expected from eqn. 9,

TABLE I

PHYSICO-CHEMICAL CONSTANTS USED IN SIMULATION (25°C)

m_0 = Absolute mobility ($cm^2/V \cdot sec$) · 10^5. pK_a = Thermodynamic acidity constant, assumed values being used for chloride and sulphamate ions. Abbreviations used for the samples are given in parentheses.

Ions	m_1	pK_1	m_2	pK_2
Buffers				
β-Alanine	36.7*	3.552		
ε-Aminocaproic acid	28.8*	4.373		
Creatinine	37.2*	4.828		
Histidine	29.6*	6.04		
Imidazole	52.0*	7.15		
Tris(hydroxymethyl)aminomethane	29.5*	8.076		
Amediol	29.5*	8.78		
Samples				
Acetic acid (Ac)	42.4	4.756		
Adipic acid (Adi)	24.6*	4.43	52.4*	5.277
Formic acid (For)	57.1	3.796		
Iodic acid	42.0	0.77		
Lactic acid (Lac)	36.5	3.858		
Tartaric acid (Tar)	34.6*	3.036	60.5*	4.366
Maleic acid (Mal)	42.5*	1.921	62.0*	6.225
Succinic acid (Suc)	33.0*	4.207	60.9*	5.638
β-Chloropropionic acid (Cl-Pr)	36.5	4.076		
Sulphamic acid (Sul)	50.3*	−2		
Hydrofluoric acid	57.4	3.173		
Hydrochloric acid	79.08	−2		

* Isotachophoretically evaluated. The other constants were taken from the literature[4–6].

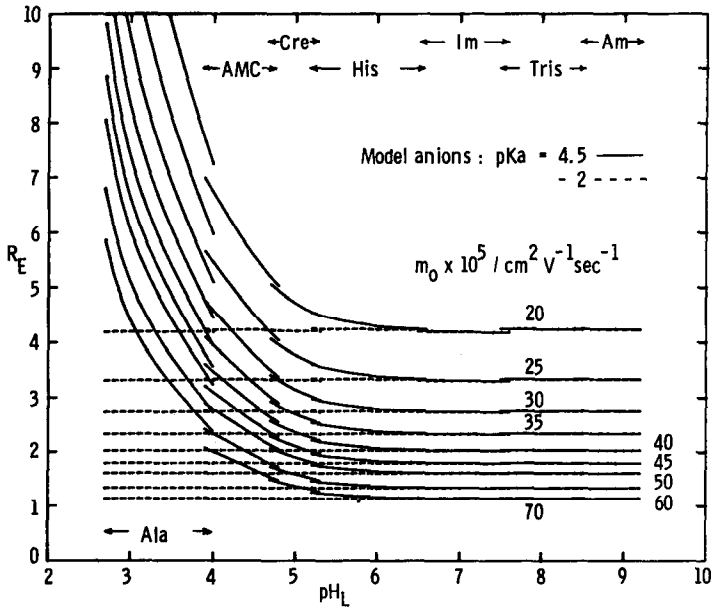

Fig. 1. Effect of pH_L on the simulated R_E values of model anions. The buffers used were β-alanine (Ala, pH_L = 2.7–4), ε-aminocaproic acid (AMC, 3.9–4.8), creatinine (Cre, 4.7–5.3), histidine (His, 5.2–6.6), imidazole (Im, 6.5–7.6), tris(hydroxymethyl)aminomethane (Tris, 7.5–8.5), and amediol (Am, 8.4–9.2). The concentration of the leading ion, Cl^-, was 0.01 *M*.

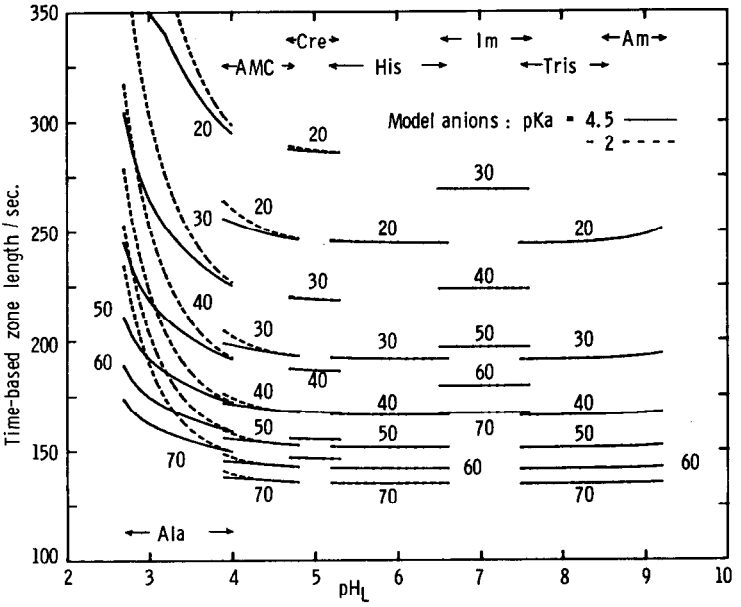

Fig. 2. Effect of pH_L and the buffers on the simulated time-based zone lengths for 100 nmol model anions. The driving current was 100 μA. For the electrolyte conditions, see Fig. 1.

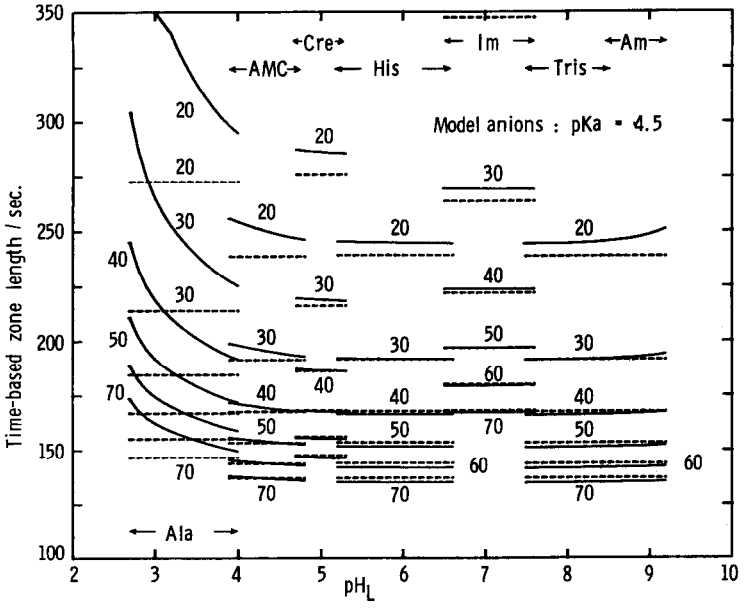

Fig. 3. Effect of pH_L and the buffers on the time-based zone lengths for 100 nmol model anions, the solid curves were accurately simulated and the broken lines were estimated by the use of the absolute mobilities of the model anions and buffers. For the electrolyte conditions, see Fig. 1.

the time-based zone length increases in proportion to the ratio m_B/m_S. Contrary to the R_E values, the zone lengths coincided for the anions with pK_a 4.5 and -2, except at pH_L below *ca.* 4, when the absolute mobilities of the buffer were the same. The differences between the zone lengths in the low pH_L range are due to differences in pH_S in zones for the anions with pK_a 4.5 and -2. The pH_S values are higher than pH_L in anionic analysis and the pH shift, $pH_S - pH_L$, is larger for the samples with $pK_a = 4.5$ than those with pK_a -2 at the same pH_L: the contributions of H^+ to κ_S of the samples with pK_a -2 are larger than those of the samples with $pK_a = 4.5$ in the low pH_L range. The small difference between the ionic strengths also contributes to the discrepancy in the low pH_L range. However, in the medium pH range it can be concluded that the time-based zone lengths are not dependent on the pK_a values of the samples, rather with the mobilities of the samples and the buffers.

In eqn. 9 m_B and m_S should be corrected for the ionic strength. To a fairly good approximation, however, they can be replaced by m_0 of the samples and the buffers. Fig. 3 shows the simulated zone lengths and the roughly estimated ones using the m_0 values. When the m_0 of the sample and the buffer are nearly equal, *e.g.*, the absolute mobility of the sample is $30 \cdot 10^{-5}$ cm^2/V · sec and the buffers are His ($m_0 = 29.6 \cdot 10^{-5}$ cm^2/V · sec) and Tris ($29.5 \cdot 10^{-5}$ cm^2/V · sec), good agreement was obtained between the simulated and the estimated values, owing to the fact that the mobilities of the sample and the buffers corrected for ionic strength are also nearly equal.

For the rough estimation of the zone lengths, a function which indicates the deviation of the roughly estimated t from the exact value may be useful. Fig. 4 shows the pH_L dependence of the deviation for the samples with $pK_a = 4.5$

$$\text{Deviation (\%)} = [t(\text{es}) - t(\text{ex})] \cdot 100/t(\text{ex}) \quad (20)$$

where t(ex) and t(es) are exact and the roughly estimated time-based zone lengths.

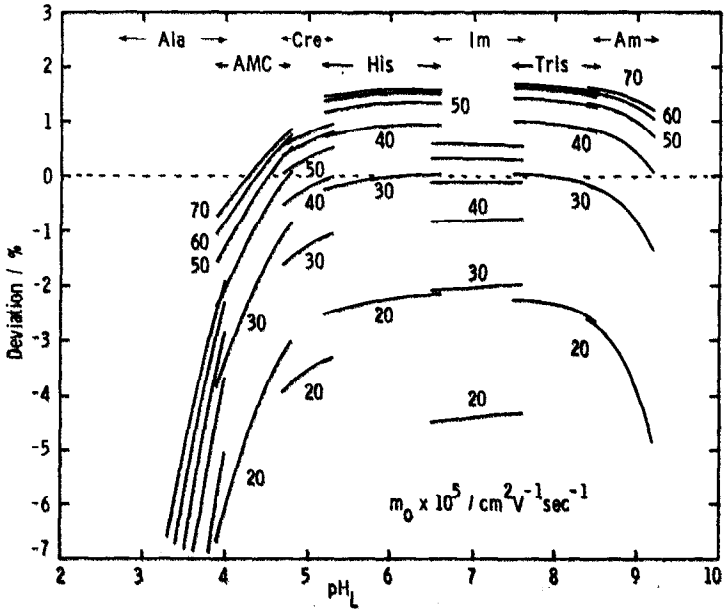

Fig. 4. The deviations (%) between the accurately evaluated and the estimated time-based zone lengths for the model anions with $pK_a = 4.5$. For the electrolyte conditions, see Fig. 1.

Apparently, the error is at maximum of 6% at pH_L above 4. Even when the pK_a of a sample is as low as -2 (not shown in Fig. 4), the deviation did not exceed 5%, when $pH_L > ca.$ 4.5. When the pH_L range is limited to 4.5–8.5 and the samples are limited to $pK_a > 2$ with $m_0 > 25 \cdot 10^{-5}$ cm²/V · sec, the deviation is within ± *ca.* 3% except for the Im buffer, confirming the utility of the simple eqn. 9. When $pH_L < 4.5$ and > 8.5, the deviation becomes larger owing to the increasing contribution of H^+ or OH^- to the conductivity which is not considered in eqn. 9.

For divalent anions, eqn. 16, it was concluded that pK_1 does not affect the zone lengths, when pH_L is in the medium pH range. To confirm this, the zone lengths were simulated for several divalent model anions with different pK_1 (2 and 5), fixing pK_2 at 6. The absolute mobilities of monovalent anions (m_1) were varied in the range $20–40 \cdot 10^{-5}$ cm²/V · sec and those of divalent anions (m_2) were taken as $m_1 \times 2$. The simulation conditions were the same as those used for monovalent anions. Figs. 5 and 6 show the pH_L dependence of R_E values and zone lengths, respectively. The R_E curves were again approximately continuous, on the other hand, the curves for t were apparently discontinuous, suggesting a strong effect of the m_0 of the buffer on t. In spite of the distinct difference between R_E values for samples with different pK_1 and the same mobility, the zone lengths were similar except at $pH_L < 4$. Contrary to the monovalent ions, t decreases in the low pH_L range, however, the profiles of the curves for the samples of different pK_1 were very similar, confirming that t is independent of pK_1. The reason for the slight discrepancy is as discussed for the monovalent anions.

Fig. 7 shows the pH_L dependence of the deviation of the roughly estimated zone lengths (eqns. 17 and 18) from the accurately simulated ones for several divalent model anions. The pH_S in eqn. 18 was replaced by pH_L and to compensate for this

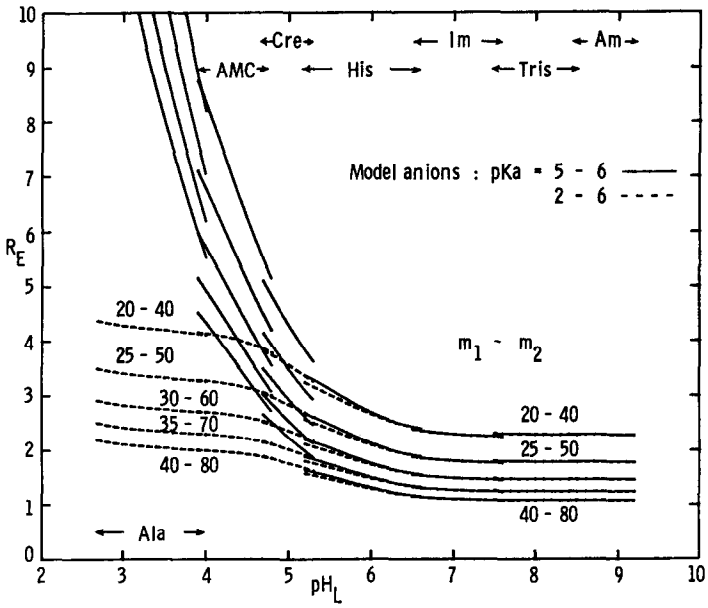

Fig. 5. Effect of pH_L and buffers on the simulated R_E values of the model divalent anions. The $m_1 - m_2$ are the absolute mobilities (cm²/V · sec) · 10^5 of the monovalent and divalent components. For electrolyte conditions, see Fig. 1.

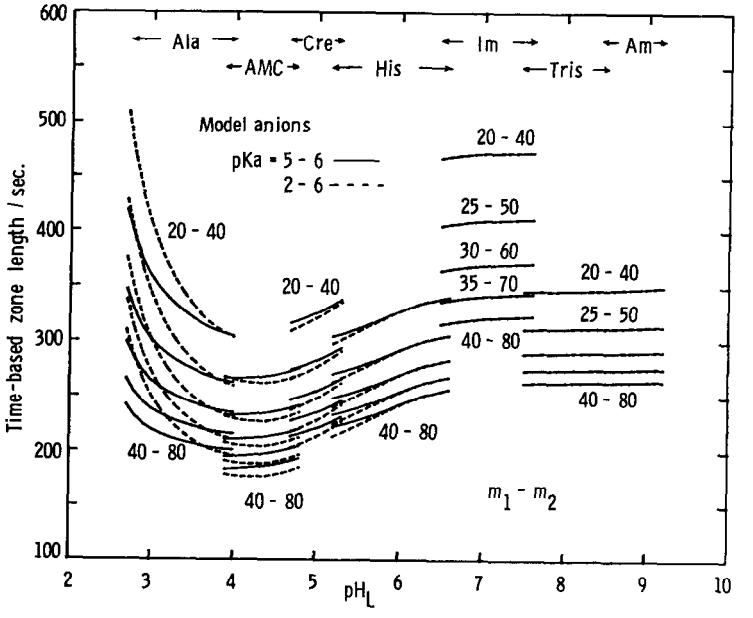

Fig. 6. Effect of pH_L and buffers on the simulated time-based zone lengths of the model divalent anions. For $m_1 - m_2$, see Fig. 5; for electrolyte conditions, see Fig. 1.

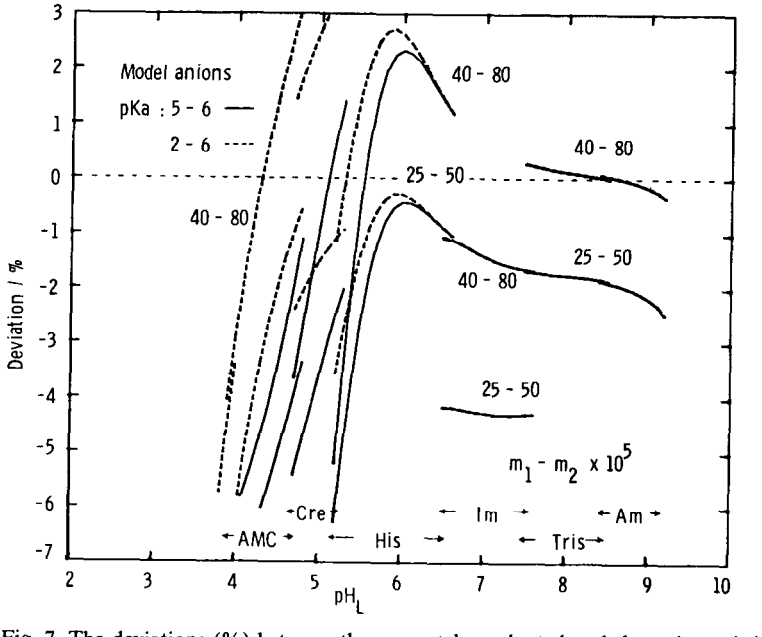

Fig. 7. The deviations (%) between the accurately evaluated and the estimated time-based zone lengths for the model anions with pK_a = 5–6 and 2–6. For the electrolyte conditions, see Fig. 1.

0.7 was used instead of 0.301 assuming the pH shift of *ca.* 0.4. At $pH_L < 6$, the deviation is strongly influenced by pH_L even for the same buffer. This is caused by the fact that $pH_S - pH_L$ is actually a variable and the shift becomes larger in the low pH_L range. For this reason, the discontinuity in the deviation upon change of buffer ion is more marked than in the case of the monovalent ions (Fig. 4). Nevertheless, the deviation was within the range +3.5 to −6% at $pH_L > 4.5$ for divalent anions with $m_1 > 25 \cdot 10^{-5}$ cm²/V · sec. The estimation can be improved if a larger value than 0.7 is employed in the lower pH_L range. When $pH_L > pK_2$, the deviation is independent of the value (0.7), since eqn. 17 can be reduced to $t = Fn(2 + m_{B,S}/m_{S,1})/I$. Thus, in this range the zone lengths are not dependent on pK_2 and pH_S.

It can be concluded that the time-based zone lengths of mono- and divalent anions can be estimated roughly using the absolute mobilities and pH_L without the aid of computer simulation. However, for accurate estimation in the wide range of pH *ca.* 3 to 10, the simulations should be carried out by taking into account the contributions of H^+ and OH^- to the conductivity and by correction of the mobilities and dissociation constants for ionic strength[1].

To confirm the general applicability of the simulation technique for quantitative analysis, several anions were considered. Beckers and Everaerts[3] measured the time-based zone lengths of acetic, adipic, formic, iodic, lactic, tartaric and maleic acids in two leading electrolytes buffered by histidine (pH_L = 6.02) and imidazole (7.05), using a thermometric detector. The zone lengths of succinic, β-chloropropionic and sulphamic acids at pH_L 6.02 and of hydrofluoric acid at pH_L 7.05 were also measured. The applied driving current was 70 μA. Simulations of the isotachophoretic equilibria were carried for these samples under the same conditions. The physico-chemical constants used are listed in Table I[4–7]. The simulated R_E values and time-based zone lengths are given in Table II for pH_L 6.02 and Table III for pH_L 7.05, and the simulated and observed zone lengths are compared in Table IV.

TABLE II

SIMULATED R_E VALUES AND TIME-BASED ZONE LENGTHS OF THE SAMPLES, EFFECTIVE MOBILITIES AND CONCENTRATIONS OF ZONE CONSTITUENTS AT pH_L 6.02 BUFFERED BY HISTIDINE (25°C)

R_E = Ratio of potential gradients, E_S/E_L; t = time-based zone length (sec) for 100-nmol samples at 70 μA; $\bar{m}_S$ = effective mobility (cm²/V · sec) · 10^5 of sample ion; pH_S = pH of sample zone; $\bar{Z}$ = apparent charge of sample; C_S^t = total concentration (mM) of sample; $C_{B,S}^t$ = total concentration (mM) of buffer; $\bar{m}_{B,S}$ = effective mobility (cm²/V · sec) · 10^5 of buffer ion; I = ionic strength × 10^3.

Sample	R_E	t	$\bar{m}_S$	pH_S	$\bar{Z}$	C_S^t	$C_{B,S}^t$	$\bar{m}_{B,S}$	I
Ac	1.98	231.5	37.7	6.140	−0.96	8.048	16.65	−12.4	7.76
Adi	1.78	431.7	41.9	6.120	−1.90	4.316	17.04	−12.5	12.1
For	1.42	206.8	52.5	6.067	−1.00	9.013	17.62	−13.4	8.97
IO_3	1.93	232.4	38.7	6.112	−1.00	8.017	16.62	−12.8	8.02
Lac	2.24	247.8	33.2	6.142	−1.00	7.520	16.13	−12.4	7.48
Tar	1.46	412.6	51.1	6.075	−1.99	4.516	17.60	−13.1	13.1
Mal	1.61	338.6	46.4	6.121	−1.52	5.503	17.42	−12.5	11.2
Suc	1.57	394.7	47.6	6.112	−1.80	4.721	17.49	−12.6	12.3
Cl-Pr	2.25	247.8	33.1	6.145	−0.99	7.520	16.13	−12.3	7.46
Sul	1.60	215.9	46.7	6.081	−1.00	8.630	17.24	−13.2	8.63

TABLE III

SIMULATED R_E VALUES AND TIME-BASED ZONE LENGTHS OF THE SAMPLES, EFFECTIVE MOBILITIES AND CONCENTRATIONS OF ZONE CONSTITUENTS AT pH_L 7.05 BUFFERED BY IMIDAZOLE (25°C)

For symbols see Tables I and II.

Sample	R_E	t	$\bar{m}_S$	pH_S	$\bar{Z}$	C_S^t	$C_{B,S}^t$	$\bar{m}_{B,S}$	I
Ac	1.91	308.7	39.1	7.181	−1.00	7.346	14.51	−24.6	7.32
Adi	1.69	572.4	44.3	7.158	−1.99	3.962	15.07	−25.1	11.8
For	1.41	264.0	52.9	7.113	−1.00	8.593	15.76	−26.4	8.59
IO_3	1.92	310.5	38.9	7.180	−1.00	7.306	14.47	−24.6	7.31
Lac	2.22	338.1	33.6	7.216	−1.00	6.708	13.87	−23.6	6.71
Tar	1.44	529.5	51.9	7.123	−2.00	4.283	15.73	−26.0	12.8
Mal	1.43	509.9	52.2	7.129	−1.92	4.448	15.79	−25.9	12.6
F	1.39	262.1	53.7	7.110	−1.00	8.653	15.81	−26.5	8.65

TABLE IV

OBSERVED* AND SIMULATED TIME-BASED ZONE LENGTHS OF SEVERAL ANIONS AT pH_L 6.02 (HISTIDINE BUFFER) AND 7.05 (IMIDAZOLE BUFFER)

Sample	pH_L = 6.02				pH_L = 7.05			
	Sample amount [nmol (μl)]	*Time-based zone length (sec)*			*Sample amount [nmol (μl)]*	*Time-based zone length (sec)*		
		Obs.	*Calc.*	*Dev. (%)*		*Obs.*	*Calc.*	*Dev. (%)*
Ac	150 (3)	358.5	347.3	−3.1	150 (3)	467	463.1	−0.8
	100 (2)	234	232.5	−0.6	100 (2)	308	308.7	0.2
	50 (1)	120	115.8	−3.5	50 (1)	154	154.4	0.3
Adi	75 (3)	335	323.8	−3.3	75 (3)	407	429.3	5.5
	50 (2)	223	215.9	−3.2				
For	150 (3)	311	310.1	−0.3	150 (3)	398	395.9	0.5
	50 (1)	105	103.4	−1.5	100 (2)	255	264.0	3.5
					50 (1)	129	132.0	2.3
IO_3	150 (3)	350	348.7	−0.4	150 (3)	465	465.7	0.2
	100 (2)	231	232.4	0.6				
Lac	93 (3)	222	230.4	3.8	102.9 (3)	340	347.9	2.3
Tar	75 (3)	320	309.5	−3.3	75 (3)	416	397,.1	−4.5
	50 (2)	213	206.3	−3.1				
Mal	100 (2)	349	338.6	−3.0	150 (3)	735	746.8	4.1
					100 (2)	491	509.9	3.8
Suc	40 (4)	163	157.9	−3.3				
	30 (3)	119	118.4	−0.5				
Sul	150 (3)	335	323.9	−3.3				
F					150 (3)	409	393.2	−3.9

* By Beckers and Everaerts[3]; the driving current was 70 μA.

TABLE V

OBSERVED* AND SIMULATED COEFFICIENTS OF CALIBRATION LINE [n (nmol) = A t(sec) + B] AT pH_L 6.02 AND 7.05

Sample	pH_L = 6.02			pH_L = 7.05		
	Obs.		*Calc.*	*Obs.*		*Calc.*
	A	*B*	*A*	*A*	*B*	*A*
Ac	0.419	0.48	0.432	0.319	1.07	0.324
Adi	0.223	0.22	0.232	–	–	–
For	0.485	−0.97	0.484	0.371	3.23	0.379
IO_3	0.420	2.94	0.430	–	–	–
Tar	0.234	0.23	0.242	–	–	–
Suc	0.227	2.96	0.253	–	–	–
Mal	–	–	–	0.205	−0.62	0.196

* The values were obtained by the least-squares method using the observed zone lengths[3]. The driving current was 70 μA.

At pH_L 6.02, the mean error between the calculated and the observed zone lengths was 2.2%, and at pH_L 7.05 the error was 2.5%, supporting the validity of the simulations. From the deviations between the calculated and the observed zone lengths at pH_L 6.02, the error in an observation might be less than a few per cent, suggesting that the mean errors in the simulations were comparable to the errors in observation. Strictly speaking, the simulated zone lengths at pH_L 6.02 were underestimated, except for lactate ion. This might suggest that the actual mobility of histidine buffer is slightly higher than the used value of $29.6 \cdot 10^{-5}$ cm^2/V · sec, evaluated isotachophoretically in our laboratory by analysing R_E values. For lactate ion, the zone lengths were overestimated at pH_L 6.02 and 7.05, therefore, the actual m_0 of lactate ion might be larger than the value employed. For maleate and adipate ions, the mobilities employed might be slightly different from the actual ones. Table V summarizes the evaluated gradients of the calibration lines on the basis of the observed time-based zone lengths, compares them with the time simulated ones. Satisfactory agreement was achieved.

Beckers and Everaerts[3] proposed a calibration constant, K_{cal}, characteristic of all ionic species in a chosen system:

$$K_{cal} = 1000\, n/C_S^t\, t \tag{21}$$

Inserting eqn. 6 into eqn. 21 we obtain:

$$K_{cal} = \pi r^2 v = \pi r^2 E_L \bar{m}_L = \frac{1000\, I}{C_L^t F} \cdot \frac{m_L}{m_L + m_{B,L}} \tag{22}$$

Namely, K_{cal} is the volume of an isotachophoretically migrating zone in unit time (cm^3/sec), which depends on the migrating velocity and the inner radius of the cap-

illary tube used. The calculated mean values of K_{cal} using observed zone lengths and simulated concentrations were reported[3] as $4.985 \cdot 10^{-5}$ for the electrolyte system of pH_L 6.02 and $4.365 \cdot 10^{-5}$ for that of pH_L 7.05 under a driving current of 70 μA. In the present work, the calculated mean values of K_{cal} were $5.278 \cdot 10^{-5}$ and $4.451 \cdot 10^{-5}$ respectively for the two electrolyte systems. The difference between the two sets of K_{cal} values can be attributed to the difference in the simulated sample concentrations: in the present simulations, m_0 and pK_a were corrected to a finite ionic strength. By the use of eqn. 22, the inner radius of the capillary used can be estimated, if the isotachophoretic velocity, v, is available. The simulated v in the first electrolyte system was $2.7332 \cdot 10^{-2}$ cm/sec and that in the second was $2.2456 \cdot 10^{-2}$ cm/sec. The I.D. values thus estimated were 0.496 mm and 0.502 mm for the two systems. On the other hand, the values estimated using the reported K_{cal} were 0.482 mm and 0.497 mm, respectively. The I.D. values estimated for the different electrolyte systems should coincide with each other. The agreement was satisfactory in the present work, confirming again the validity of the present determinations.

Fig. 8 shows the pH_L dependence of the simulated R_E values of actual samples. The simulation conditions were the same as those used for model anions. Except for iodate, sulphamate and maleate with small pK_a, the R_E values rapidly increase in the low pH_L range. Apparently, the actual samples may not be completely separated at any pH_L. It is probable that the reported zone lengths have been measured individually or for a few groups. Fig. 9 shows the pH_L dependence of the simulated time-based zone lengths. The driving current was 100 μA. The zone lengths of the monovalent anions are constant in the pH_L range buffered by the same kind of counter ion, except for $pH_L < 4$. The overlapping of the curves is due to several monovalent

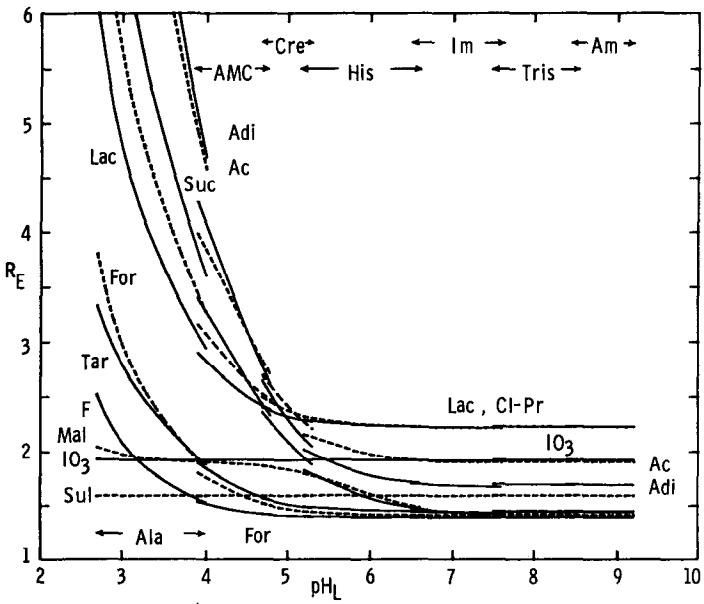

Fig. 8. Effect of pH_L and buffers on the simulated R_E values of several actual samples: adipate (Adi); acetate (Ac); succinate (Suc); lactate (Lac); β-chloropropionate (Cl-Pr); formate (For); tartrate (Tar); fluoride (F); iodate (IO_3); maleate (Mal) and sulphamate (Sul). For electrolyte conditions, see Fig. 1.

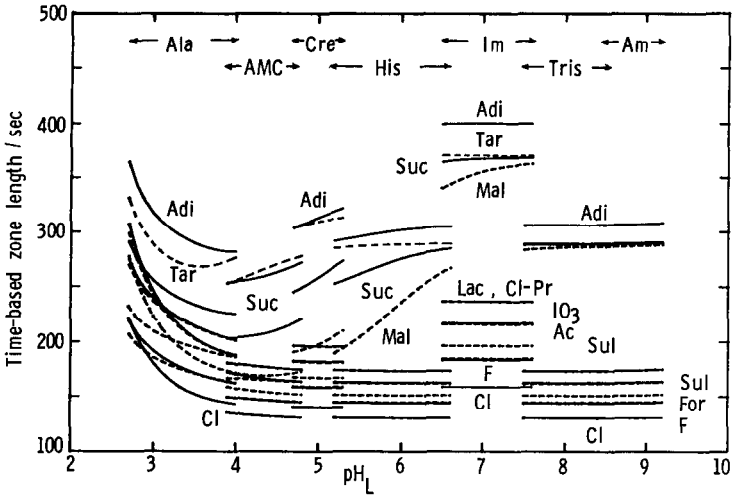

Fig. 9. Effect of pH_L and buffers on the simulated time-based zone lengths of the samples in Fig. 8. The applied current was 100 μA. For the electrolyte conditions, see Fig. 1.

anions with similar absolute mobilities. The zone lengths of divalent anions vary with pH_L, even when the same buffer is used, except at high pH_L. This fact can be utilized for the experimental discrimination of the monovalent and multivalent ions. In Fig. 9 the zone lengths for chloride ion are also shown. When the amount of the leading ion loaded in a separating compartment is known, the time for detection of the first sample zone can be estimated.

Thus, the practical utility of the proposed simulation technique in determinations is confirmed. This technique also enables determination without the use of a conventional calibration curve when the separation is complete. At present, the reproducibility of the observed zone lengths is within a few per cent. When the accuracy of the absolute mobilities on the samples and buffers is improved, more exact determinations may be possible.

Indices such as R_E have been used for qualitative analysis. However, a quantitative index, the time-based zone lengths, can also be utilized for qualitative analysis, since the zone length under electrolyte conditions is another characteristic of a sample. Moreover, for the evaluation of absolute mobility, pK_a and stability constants, the observed time-based zone lengths can be analysed by the least-squares method together with the R_E values.

REFERENCES

1 T. Hirokawa and Y. Kiso, *J. Chromatogr.*, 242 (1982) 227.
2 T. Hirokawa and Y. Kiso, *J. Chromatogr.*, 257 (1983) 197.
3 J. L. Beckers and F. M. Everaerts, *J. Chromatogr.*, 71 (1972) 329.
4 R. A. Robinson and R. H. Stokes, *Electrolyte Solutions*, Butterworths, London, 2nd ed., 1959.
5 Landolt-Bornstein, *Zahlenwerte und Funktionen*, Part II; Vol. 7, Springer, Berlin, 6th ed., 1960.
6 *International Critical Tables of Numerical Data, Physics, Chemistry and Technology*, Vol. VI, McGraw-Hill, New York, London, 1933.
7 T. Hirokawa, M. Nishino and Y.Kiso, *J. Chromatogr.*, 252 (1982) 49.